JOURNAL OF Materials CHEMISTRY

Polymorphism in nickel hydroxide: role of interstratification

Michael Rajamathi,[a] P. Vishnu Kamath[a] and Ram Seshadri[b]

[a]*Department of Chemistry, Central College, Bangalore University, Bangalore 560 001, India. E-mail: vishnu@sscu.iisc.ernet.in*
[b]*Solid State and Structural Chemistry Unit, Indian Institute of Science, Bangalore 560 012, India*

Received 13th July 1999, Accepted 4th November 1999

In addition to the well-known α and β modifications, nickel hydroxide is shown to exist in a number of poorly crystalline forms—clearly distinguishable by their signature X-ray powder diffraction patterns. DIFFaX simulations combined with compositional analysis and IR spectral data indicate that these are interstratified phases consisting of α- and β-type structural motifs intermixed in varying proportions.

Introduction

Nickel hydroxide is the positive electrode material in all nickel-based alkaline secondary cells.[1] Considerable work has been done to understand the relationship between the structural features and the charge storage capacity of nickel hydroxide.[2–5] Nickel hydroxide exhibits polymorphism and two forms, namely α and β, are well documented.[6]

Nickel hydroxide obtained by alkali precipitation from a nickel salt solution followed by hydrothermal treatment is a crystalline stoichiometric material with the formula $Ni(OH)_2$.[7] This form is known as β-nickel hydroxide and is isostructural with the mineral brucite, $[Mg(OH)_2]$ (space group $P\bar{3}m1$, $a=3.12$, $c=4.6$ Å).[8] In this structure, the OH^- ions are hexagonally packed and the Ni^{2+} ions occupy alternate rows of octahedral sites leading to a layered structure which can be described as an ordered stacking of charge neutral layers of composition $[Ni(OH)_2]$.

Nickel hydroxide obtained by precipitation using ammonia[9] or by electrosynthesis[10] is a poorly ordered material and is denoted α-nickel hydroxide. It is hydroxyl deficient and can be formulated as $Ni(OH)_{2-x}(A^{n-})_{x/n}\cdot mH_2O$ where $A^{n-}=Cl^-$, AcO^-, NO_3^- or SO_4^{2-}, $x=0.15$–0.20 and $m=0.66$–0.75.[9,11] α-Nickel hydroxide comprises positively charged layers of composition $[Ni(OH)_{2-x}(H_2O)_x]^{x+}$ which intercalate anions for charge balance. This leads to an increased interlayer spacing ($c=7.6$ Å when $A^{n-}=NO_3^-$). Also, the slabs are oriented randomly with respect to one another, leading to turbostratic disorder.[9]

In addition to these well-known forms, a few other modifications of nickel hydroxide have also been reported. By *chimie douce* methods, involving hydrolysis of $NaNiO_2$ followed by reduction, an ordered phase of nickel hydroxide, formulated as $Ni(OH)_2\cdot 0.75H_2O$ and whose interlayer spacing matches with that of the α form has been prepared.[12] This material is known as α*-nickel hydroxide. Nickel hydroxide obtained by ambient temperature alkali precipitation from a nickel salt solution or by aging α-nickel hydroxide in an alkali exhibits an X-ray powder diffraction (XRPD) pattern similar to that of β-nickel hydroxide, but is poorly ordered. This phase has been referred to as β_{bc}-nickel hydroxide (bc: badly crystalline) in the literature.[13] We have recently reported a new phase of nickel hydroxide, which is an interstratification of α- and β-type motifs.[14] This phase will be referred to as IS-nickel hydroxide.

Most of the phases encountered in the solid state chemistry of nickel hydroxide are poorly ordered, but the XRPD pattern of each phase has characteristic signature features. The poorly ordered phases and the minor variations between them can be better understood with the help of XRPD simulation studies. The DIFFaX computer program provides a powerful tool for simulating XRPD patterns of layered materials with stacking faults, turbostratic disorder and interstratification.[15] In this paper we compare the various forms of nickel hydroxide, using X-ray powder diffraction in conjunction with DIFFaX simulations to understand the nature of structural modifications that lead to polymorphism in nickel hydroxide.

Experimental

Materials synthesis

All nickel hydroxide samples studied here were prepared from nickel nitrate solutions in order that the adsorbed/intercalated anion was the same in all cases. β-Nickel hydroxide was obtained by two different methods. One sample (β1) was obtained by adding 50 ml of 1 M nickel nitrate solution to 50 ml of 2 M NaOH solution dropwise with constant stirring, and treating the gel so obtained hydrothermally in a stainless steel autoclave at 180 °C for 48 h. The second sample (β2) was prepared by adding 20 ml of 1 M nickel nitrate solution to 100 ml of 25% ammonia solution, all in one portion, and aging the product formed in the mother liquor for 10 d. β_{bc}-Nickel hydroxide was also synthesised by two different methods. The first sample ($\beta_{bc}1$) was obtained by adding 50 ml of 1 M nickel nitrate solution to 50 ml of 2 M NaOH solution dropwise with constant stirring at room temperature. The second sample ($\beta_{bc}2$) was prepared by aging nickel hydroxynitrate, $Ni_3(OH)_4(NO_3)_2$, in 6 M KOH for one month. Two different samples of α-nickel hydroxide, α1 and α2, were obtained by cathodic reduction of an aqueous 1 M nickel nitrate solution at a current density of 1.5 mA cm^{-2} at 60 and 25 °C, respectively.[16] Other nickel hydroxide samples were synthesised by adding a 2 M solution of NaOH to 50 ml of 1 M nickel nitrate solution with constant stirring until the reaction mixture pH attained values in the range 6–9. These samples are designated as α_{am} (am: amorphous) for reasons discussed later. IS-nickel hydroxide was obtained by an alkali precipitation procedure as described elsewhere.[14] In all cases the products were washed thoroughly with deionised water, filtered and dried at 65 °C to constant weight.

Characterization

The samples were characterized by X-ray powder diffraction (JEOL JDX8P powder X-ray diffractometer, Cu-Kα,

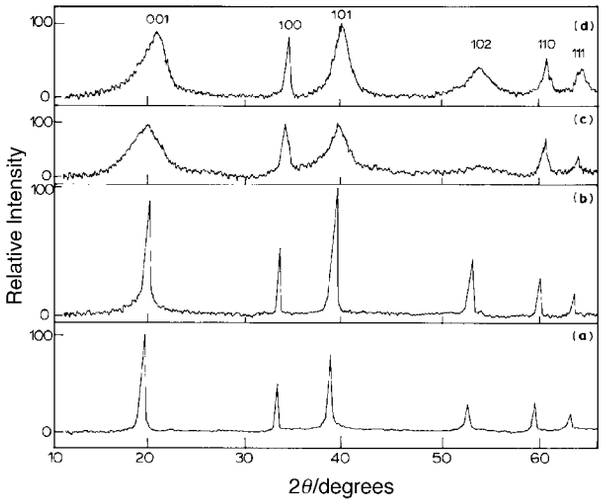

Fig. 1 XRPD patterns of the nickel hydroxide samples β1 (a), β2 (b), $\beta_{bc}1$ (c) and $\beta_{bc}2$ (d).

$\lambda = 1.541$ Å), infrared spectroscopy (Nicolet Model Impact 400D FTIR spectrometer, KBr pellets, 4 cm^{-1} resolution) and thermogravimetry (lab-built system, heating rate: 5 °C min^{-1}).

Selected samples were subjected to wet chemical analysis. The nickel content was estimated by gravimetry and the hydroxyl content was estimated by pH metric titrations, as described elsewhere.[17] In the case of samples with hydroxyl deficiencies, an equivalent anion (nitrate) content was assumed for charge neutrality. The unaccounted weight was attributed to adsorbed/intercalated water. The approximate formulae thus obtained were verified by thermogravimetry.

XRPD simulation studies

Simulation studies were carried out using the code DIFFaX (Version 1.8.1).[15] The atomic positions in the NiO_2 layers were obtained from the literature.[18] A Lorentzian broadening was assumed for the sake of simplicity.

Results and discussions

In Fig. 1 the XRPD patterns of the β- and β_{bc}-nickel hydroxide samples are shown. The β samples [Fig. 1(a) and (b)] are characterized by sharp reflections [fwhm of the (001) reflection = 0.3°] at 4.6, 2.7, 2.33, 1.75, 1.56 and 1.48 Å. The pattern of β2 [Fig. 1(b)] differs from that of β1 [Fig. 1(a)] in the relative intensities of the (001) and (101) reflections. While for β1 the (001) peak is the most intense, for β2 the (101) peak is the most intense.

The two β_{bc} samples reported here [Fig. 1(c) and (d)] show the following characteristics in their XRPD patterns:

(1) The *d*-spacings are similar to those of their crystalline counterparts.
(2) Although all the reflections are broad, as expected of badly crystalline materials, the (100) and (110) reflections are relatively sharper [fwhm of (001) reflection = 2.8°, but fwhm of (100) reflection = 0.5°].
(3) The two β_{bc} samples differ from each other in the relative intensities of their (102) reflections.

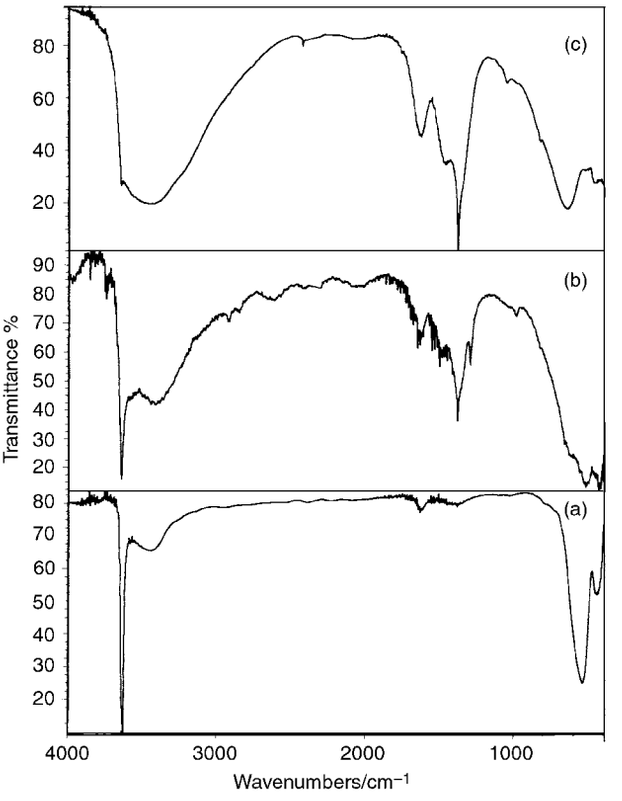

Fig. 2 IR spectra of the nickel hydroxide samples β1 (a), $\beta_{bc}1$ (b) and α1 (c).

Delmas and Tessier have recently suggested that the broadening of all non-*hk*0 reflections in β_{bc}-nickel hydroxide are due to stacking faults.[19] Although a reasonable extent (*ca.* 20%) of stacking faults in conjunction with suitable pseudo-Voigt broadening leads to a pattern similar to that of β2 [Fig. 1(b)], even a very large extent of these faults (> 80%) fails to simulate patterns that match those of $\beta_{bc}1$ and $\beta_{bc}2$ [Fig. 1(c) and (d)].

Interstratification, which leads to a poorly defined *c*-parameter, is also expected to broaden the non-*hk*0 reflections selectively. Our wet chemical analyses (see Table 1) indicate that the β_{bc} samples are hydroxyl deficient, suggesting that these might be interstratified materials with low percentages of α motifs.

The idea that β_{bc} samples may be interstratified is further supported by the infrared spectroscopic data. In Fig. 2 the infrared spectra of α1 and β1, along with those of the β_{bc} samples, are shown. β-Nickel hydroxide [Fig. 2(a)] is characterized by a sharp absorption at 3650 cm^{-1} due to non-hydrogen bonded hydroxyl groups, the absence of any

Table 1 Wet chemical analyses of the nickel hydroxide samples

Sample	Weight percentage				TG weight loss (%)[a]	Approximate formula
	Ni^{2+}	OH^-	NO_3^-	H_2O		
β1	63.02	36.52	—	—	19.6 (19.4)	$Ni(OH)_2$
$\beta_{bc}1$	55.64	31.02	4.11	9.22	26.7 (29.2)[b]	$Ni(OH)_{1.93}(NO_3)_{0.07}\cdot 0.54H_2O$
α1	52.42	26.70	13.29	7.58	33.8 (33.4)	$Ni(OH)_{1.76}(NO_3)_{0.24}\cdot 0.48H_2O$
α_{am}	46.54	21.89	18.68	12.89	40.7 (39.2)	$Ni(OH)_{1.62}(NO_3)_{0.38}\cdot 0.90H_2O$
IS	48.85	25.98	8.44	16.73	37.6 (32.6)[b]	$Ni(OH)_{1.84}(NO_3)_{0.16}\cdot 1.10H_2O$

[a]Expected weight losses are shown in parentheses. [b]Deviations from the expected losses may be due to carbonate contamination.

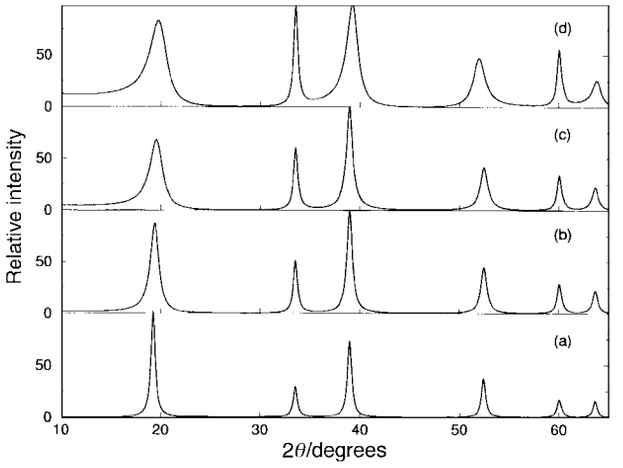

Fig. 3 Simulated XRPD patterns of β-nickel hydroxide randomly interstratified with 0 (a), 5 (b), 10 (c) and 15% (d) α motifs.

absorption due to anions in the region 1500–1000 cm^{-1} and absorptions at 540 and 470 cm^{-1} due to M–O–H bending and M–O stretching vibrations. α-Nickel hydroxide [Fig. 2(c)] exhibits a very broad absorption centered around 3500 cm^{-1}, indicative of hydrogen bonded hydroxyl groups, absorptions around 1380 cm^{-1} due to intercalated nitrate ions and M–O related vibrations at 640 and 470 cm^{-1}. β_{bc}-Nickel hydroxide, $\beta_{bc}1$ [Fig. 2(b)], exhibits the absorptions seen in the case of β-nickel hydroxide as well as α-nickel hydroxide. Here we observe a sharp peak at 3650 cm^{-1} along with a weak broad peak centered around 3500 cm^{-1} and absorptions around 1380 cm^{-1} due to intercalated nitrate ions. In the low wavenumber region we observe intense peaks at 540 and 470 cm^{-1}, along with a weak shoulder at 640 cm^{-1}. These observations further confirm that the β_{bc}-nickel hydroxide is an interstratified phase with a low percentage of α motifs.

In order to confirm the interstratification model for β_{bc}-nickel hydroxide, we simulated XRPD patterns with interstratification of a small percentage of α motifs with β motifs. Fig. 3 shows the simulated patterns with various percentages of α motifs, ranging from 0 to 15. When no α motifs are incorporated, the simulated pattern [Fig. 3(a)] agrees well with that of the crystalline β1 sample. Even a very small percentage of α motifs (5%) alters the pattern considerably, and the calculated pattern [Fig. 3(b)] matches well with that of β2 [Fig. 1(b)]. As we increase the percentage of α motifs, the non-*hk*0 peaks broaden gradually and at around 15% [Fig. 3(d)] the calculated pattern matches with the pattern of $\beta_{bc}2$ [Fig. 1(d)]. Applying a larger Lorentzian broadening (>1°) yields the pattern of $\beta_{bc}1$. Thus we have established that β_{bc}-nickel hydroxide is indeed an interstratified material with a low percentage of α motifs.

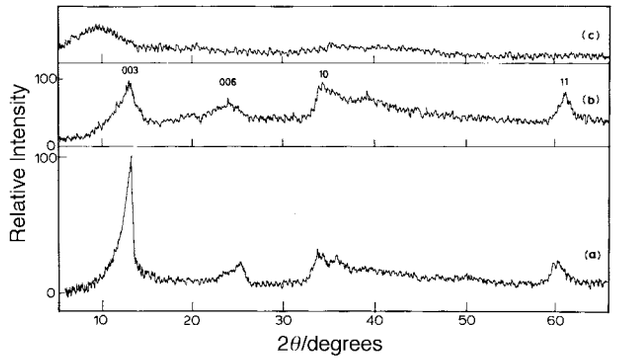

Fig. 4 XRPD patterns of the α-nickel hydroxide samples, α1- (a), α2- (b) and α_{am}-nickel hydroxide (c).

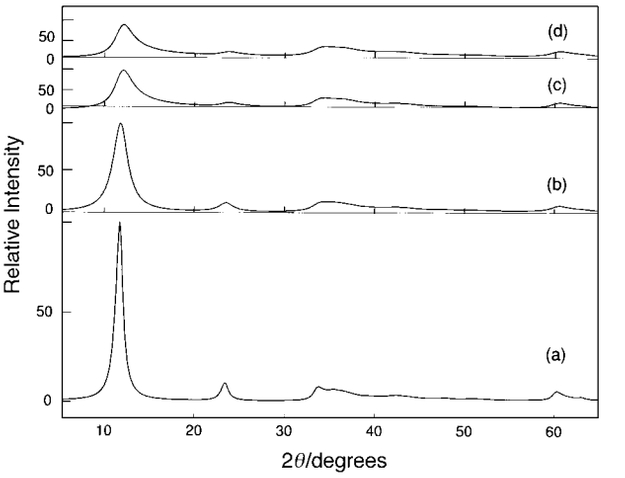

Fig. 5 Simulated XRPD patterns of α-nickel hydroxide with turbostratic stacking and various Lorentzian broadenings (L) and disc radii (R): $L=1.0°$ and $R=\infty$ (a), $L=2.0°$ and $R=\infty$ (b), $L=2.0°$ and $R=1000$ Å (c) and $L=2.0$ and $R=500$ Å (d).

Even within the α-nickel hydroxide samples we observe minor variations in XRPD patterns. Fig. 4 shows the XRPD patterns of α (α1 and α2) and α_{am}-nickel hydroxide. α-Nickel hydroxide [Fig. 4(a) and (b)] is characterized by a low angle reflection indicating a higher basal spacing of *ca.* 7.6 Å, followed by another at half this value and 'saw-tooth' shaped asymmetric bands in the regions $2\theta=32$–$45°$ and $2\theta=58$–$65°$. Although these bands are believed to indicate turbostratic disorder, no attempt has so far been made to prove this point by simulation studies.

By using stacking vectors of the form $[r_1, r_2, R_z]$, where r_1 and r_2 are random numbers ($0 \leqslant r \leqslant 1$) and R_z is the stacking distance along the c-axis, we have simulated the pattern of a turbostratically disordered nickel hydroxide with an interlayer spacing of 7.6 Å [Fig. 5(a)]. It can be seen that this pattern matches well with the observed pattern (α1) indicating that α-nickel hydroxide is indeed turbostratic.

The diffraction patterns of α1 and α2 [Fig. 4(a) and (b)] are quite similar, except that in α2 the (003) peak is very broad and the (006) peak is almost invisible. This can be attributed to either; (a) broadening due to smaller particle size and/or large Lorentzian line widths, or (b) disorder arising out of interstratification with low percentages of β motifs, since here again the peaks affected are the non-*hk*0 peaks.

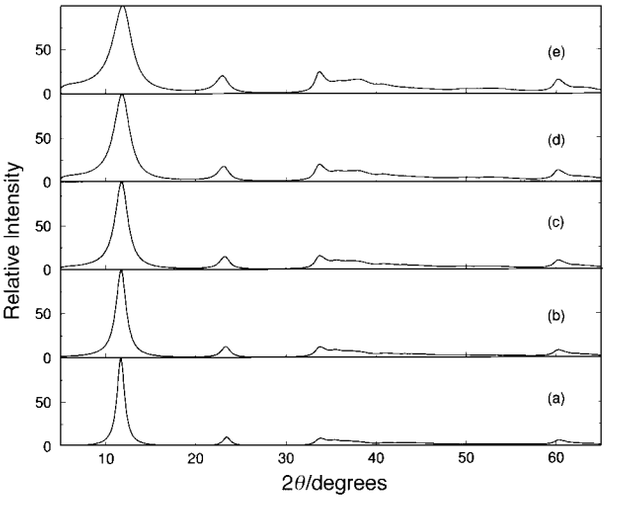

Fig. 6 Simulated XRPD patterns of α-nickel hydroxide randomly interstratified with 0 (a), 5 (b), 10 (c), 15 (d) and 20% (e) β motifs.

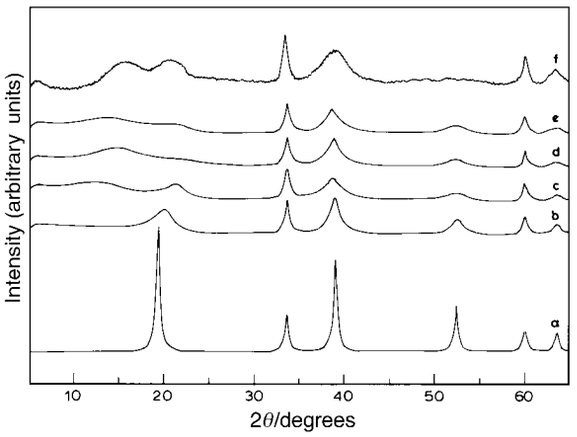

Fig. 7 Observed XRPD pattern of IS-nickel hydroxide (f) compared with the simulated XRPD patterns of β-nickel hydroxide randomly interstratified with 0 (a), 20 (b) and 40% (c) α motifs, with 40% α′ motifs (d) and 20% each α and α′ motifs (e).

Fig. 5 also shows the simulated patterns of α-nickel hydroxide with various Lorentzian broadenings and disc radii. It can be seen that the Lorentzian (2.0) and disc radius (1000 Å) needed to produce a pattern [Fig. 5(c)] that matches well with the broadening observed in α2 [Fig. 4(b)] also cause the *hk* bands to lose their saw-tooth shape. This suggests that the broadening of the (00*l*) peaks in the case of α2 is not for these reasons alone.

In Fig. 6 the simulated XRPD patterns of α-nickel hydroxide interstratified with low percentages of β motifs are shown. It can be seen that the 00*l* peaks broaden with the increasing percentage of β motifs, and for 20% β motifs we get a pattern [Fig. 6(e)] which is comparable to the pattern observed for α2 [Fig. 4(b)].

The nickel hydroxide that corresponds to the XRPD pattern shown in Fig. 4(c) is compositionally similar to α-nickel hydroxide (see Table 1). As this phase is precipitated at a relatively low pH (6–9), the comparative non-availability of hydroxyl ions results in the formation of a hydroxyl-deficient material. The IR spectrum of this sample (not shown here) is identical to that of the α form [Fig. 2(c)]. However, it is X-ray amorphous and hence we refer to it as α_{am}-nickel hydroxide (am: amorphous).

IS-nickel hydroxide exhibits an XRPD pattern [Fig. 7(f)] similar to the patterns observed for interstratified phases in layered double hydroxides.[20] Here the first peak appears at 5.6 Å, which is intermediate between the values of 4.6 Å (interlayer spacing in β-nickel hydroxide) and 7.6 Å (interlayer spacing in α-nickel hydroxide). The second peak appears at 4.2 which is between 4.6 and 3.8 Å (d_{006} of α-hydroxide). The rest of the pattern is similar to that of β_{bc}-nickel hydroxide. We have previously claimed that this material is interstratified without the benefit of simulation studies.[14] We report here the results of such simulations.

Fig. 7(a)–(c) show calculated patterns with increasing percentages of α motifs. Although the general appearance of the pattern with 40% α motifs [Fig. 7(c)] matches well with the observed pattern [Fig. 7(f)], the position of the first peak does not match with that in the experimental pattern. This problem can be overcome by using α motifs with a lower basal spacing of 7.0 Å. Such motifs, which we shall call α′ motifs, are α motifs without the intercalated water molecules. Fig. 7(d) gives the simulated pattern with 40% α′ motifs. This pattern is also not satisfactory, because although the first peak matches well with the observed pattern, the position of the second peak does not. A combination of both α and α′ motifs are required to be interstratified with β motifs in order to get a good match. The pattern calculated with 20% α motifs and 20% α′ motifs [Fig. 7(e)] compares well with the observed pattern. Therefore we conclude that IS-nickel hydroxide is a random interstratification of three kinds of motifs, namely, α, dehydrated α (α′) and β.

In conclusion, we have shown that nickel hydroxide can be obtained with various degrees of interstratification, in addition to the well known β and α forms. The realization that poorly ordered β and α forms are indeed interstratified phases throws up the possibility that α-nickel hydroxide ages to the β form through a series of interstratified intermediates. This in turn suggests that the aging process may occur through a topotactic anion leaching mechanism.

Acknowledgements

P.V.K. thanks the Department of Science and Technology, Govt. of India for financial support.

References

1 S. U. Falk and A. J. Salkind, *Alkaline Storage Batteries*, Wiley, New York, 1969.
2 M. V. Vazquez, M. J. Avena and C. P. De Pauli, *Electrochim. Acta*, 1995, **40**, 907.
3 A. Delahaye-Vidal, B. Beaudoin, N. Sac-Epée, K. Tekaia-Elhsissen, A. Audemer and M. Figlarz, *Solid State Ionics*, 1996, **84**, 239.
4 M. C. Bernard, M. Kaddam, H. Takenouti, P. Bernard and S. Senyarich, *J. Electrochem. Soc.*, 1996, **143**, 2447.
5 Min-Senk Kim, Tai-Sup Hwang and Kwang-Bum Kim, *J. Electrochem. Soc.*, 1997, **144**, 1537.
6 P. Oliva, J. Leonardi, J. F. Laurent, C. Delmas, J. J. Braconnier, M. Figlarz, F. Fievet and A. De Guibert, *J. Power Sources*, 1982, **8**, 229.
7 F. Fievet and M. Figlarz, *J. Catal.*, 1975, **39**, 350.
8 JCPDS PDF No. 14-117.
9 S. Le Bihan, J. Guenot and M. Figlarz, *C. R. Acad. Sci., Ser. C*, 1970, **270**, 2131.
10 R. S. McEwen, *J. Phys. Chem.*, 1971, **75**, 1782.
11 P. Vishnu Kamath, G. H. A. Therese and J. Gopalakrishnan, *J. Solid State Chem.*, 1997, **128**, 38.
12 J. J. Braconnier, C. Delmas, C. Fouassier, M. Figlarz, B. Beaudouin and P. Hagenmuller, *Rev. Chim. Miner.*, 1984, **21**, 496.
13 C. Faure, C. Delmas and C. Fouassier, *J. Power Sources*, 1991, **35**, 279.
14 M. Rajamathi, G. N. Subbanna and P. Vishnu Kamath, *J. Mater. Chem.*, 1997, **7**, 2293.
15 M. M. J. Treacy, J. M. Newsam and M. W. Deem, *Proc. R. Soc. London A*, 1991, **433**, 499.
16 R. S. Jayashree and P. Vishnu Kamath, *J. Appl. Electrochem.*, 1999, **29**, 449.
17 M. Dixit, G. N. Subbanna and P. Vishnu Kamath, *J. Mater. Chem.*, 1996, **6**, 1429.
18 H. D. Megaw, *Crystal Structures, A Working Approach*, W. B. Saunders, Philadelphia, 1973.
19 C. Delmas and C. Tessier, *J. Mater. Chem.*, 1997, **7**, 1439.
20 L. Guerlou-Demourgues, C. Denage and C. Delmas, *J. Power Sources*, 1994, **52**, 269.

Paper a905651c